Radiation Physics and Chemistry 169 (2020) 107984

Contents lists available at ScienceDirect

Radiation Physics and Chemistry

journal homepage: www.elsevier.com/locate/radphyschem

The effects of radiation and experimental conditions over papain nanoparticle formation: Towards a new generation synthesis

Gabriela N. Fazolin[a], Gustavo H.C. Varca[a,*], Slawomir Kadlubowski[b], Sebastian Sowinski[b], Ademar B. Lugão[a]

[a] Nuclear and Energy Research Institute, IPEN-CNEN/SP, Av. Prof. Lineu Prestes, 2242 – Cidade Universitária, CEP 05508-000 São Paulo, SP, Brazil
[b] Institute of Applied Radiation Chemistry, IARC, Lodz University of Technology, Wroblewskiego 15, 93-590 Lodz, Poland

ARTICLE INFO

Keywords:
Nanoparticle
Papain
Gamma radiation
Crosslinked enzyme
Proteolytic activity
Irradiation conditions

ABSTRACT

Papain is a natural enzyme extracted from the fruit of *Carica papaya* Linnaeus, successfully applied in the pharmaceutical area as a drug carrier and debridement agent for wounds. In recent studies papain nanoparticles were synthesized and crosslinked with the use of ionizing radiation in the search for biopharmaceutical advantages as well as the development of bioactive nanocarriers. This study addresses the effects of buffer molarity and irradiation conditions on papain nanoparticles formation. Nanoparticles were synthesized on ice bath using ethanol (20%, v/v) as a cosolvent and crosslinked by gamma radiation using a ^{60}Co source. Experimental variables included the synthesis in deionized water and in 1, 10, 25 and 50 mM phosphate buffer, under different temperatures of − 20 °C, 0 °C and 20 °C before and throughout the irradiation period, and using radiation dose rates of 0.8, 2, 5 and 10 kGy h^{-1} to reach the dose of 10 kGy. Proteolytic activity was quantified using Nα-benzoyl-DL-arginine-p-nitroanilide hydrochloride. Nanoparticle size and crosslinking by means of bityrosine were evaluated by dynamic light scattering and fluorescence measurements, respectively. Buffer molarity and radiation dose rate were identified to influence bityrosine formation and proteolytic activity without impacting nanoparticle size. Variations in temperature impacted bityrosine formation exclusively. Optimized conditions for papain nanoparticle synthesis were achieved using 50 mM phosphate buffer at the dose rate of 5 kGy h^{-1} and temperature of 0 °C throughout the process.

1. Introduction

In the last few decades' nanomaterials were studied for different kinds of applications mainly regarding pharmaceutical and biomedical areas as drug carriers and/or alternative options with less or null collateral effects (Lohcharoenkal et al., 2014). Protein belongs to an important group of materials recently employed at nanoscale to provide essential properties, such as ideal particle size, high biocompatibility, low toxicity (Tarhini et al., 2017) and cost among other features (Fuchs and Coester, 2010).

Within this context products and techniques have been recently developed, e.g. albumin bound paclitaxel, commercially known as Abraxane® – a chemotherapeutic medicine of highlighted interest for breast cancer (Grandishar, 2006); crosslinked enzyme aggregates (CLAE) with application in biocatalyst (Sheldon, 2011); papain-based products for biomedical applications (Singh and Singh, 2012) and many others.

The use of radiation to promote crosslinking of polymeric particles (Ulanski et al., 1998; Ulanski and Rosiak, 1999) has been demonstrated and may reduce the toxicity caused by introducing chemical crosslinkers, which are not required when radiation is applied. Generally, radiation can damage vital biomolecules such as DNA, proteins and lipids in two different ways: via the direct effect, through damaging DNA and other cellular targets, and the so-called indirect effect, through the action of free radicals generated during solvent radiolysis that attack biomolecules (Abdou and Abbas, 2009; Zarei et al., 2017).

Papain (EC 3.4.22.2) is a proteolytic enzyme used as a pharmaceutical agent in wound treatment due to its debridement and healing properties (Amri and Mamboya, 2012). The enzyme holds a total molecular weight of 23.5 kDa and is composed of 212 amino acids divided into two domains with an active site composed by cysteine, histidine and aspartic acid (Kamphuis et al., 1984). Recently, papain nanoparticles were developed using radiation to provide crosslinking as well as size control and were found to be potentially promising for biomedical applications (Varca et al., 2014a, 2014b). However, papain is a sensitive enzyme that may undergo degradation, oxidation and

* Correspondence to: Centro de Química e Meio Ambiente, Brazil.
E-mail address: varca@usp.br (G.H.C. Varca).

https://doi.org/10.1016/j.radphyschem.2018.08.033
Received 30 January 2018; Received in revised form 14 August 2018; Accepted 28 August 2018
Available online 29 August 2018
0969-806X/

hydrolysis by an exposition to drastic conditions or aqueous media over time (Kamphuis et al., 1984).

Over the years, some researches have combined the use of ionizing radiation and cosolvents to achieve protein nanoparticles (Queiroz et al., 2016). This method is an alternative route to promote intermolecular crosslinking in proteins and in the case of enzymes, particularly papain, the method allowed size control and crosslinking with preserved proteolytic activity (Varca et al., 2014a, 2014b, 2016).

In the seek for an optimized route and a better understanding towards the use of radiation to promote crosslinking in enzymes, the influence of temperature throughout the process, dose rate and buffer molarity over papain nanoparticle formation by means of size, protein crosslinking and proteolytic activity were carried out in this research.

2. Experimental

2.1. Materials

Papain 30.000 USP-U/mg (EC 3.4.22.2) was purchased from Merck (Germany). L-cysteine hydrochloride monohydrate, dimethylsulfoxide, ethanol, sodium hydroxide, acetic acid, ethylenediaminetetraacetic acid, monosodium phosphate and heptahydrate disodium phosphate were acquired from Synth (Brazil) and Nα-benzoyl-DL-arginine-p-nitroanilide hydrochloride was from Sigma-Aldrich (USA). All reagents were of analytical grade.

2.2. Methods

2.2.1. Standard nanoparticle synthesis

Papain nanoparticles were synthetized on ice bath at 10 mg mL^{-1} in 50 mM phosphate buffer in presence of 20% ethanol (v/v) and irradiated at 10 kGy under refrigerated conditions using synthetic ice as described by Varca et al. (2014a, 2014b, 2016). The samples were exposed to γ-radiation at dose rate of 5 kGy h^{-1} using ^{60}Co as radioactive source in a Multipurpose Irradiator. Samples were then filtrated using 0.45 μm cellulose acetate syringe filters (Macherey-Nagel, Germany) and stored at 4 °C to prior analysis.

Native, irradiated (10 kGy) and papain in presence of ethanol (20% v/v) were considered as controls of the nanoparticle. Dosimetry was performed using Amber Perspex 3042 (Harwell Dosimeters, UK), a dyed-polymethylmethacrylate dosimeter.

2.2.2. Effects of irradiation parameters and experimental conditions over nanoparticle synthesis

2.2.2.1. Buffer molarity. The nanoparticles were synthetized in deionized water and in phosphate buffer molarities of 1, 10, 25 and 50 mM, irradiated and handled as described for the standard nanoparticle synthesis.

2.2.2.2. Radiation dose rate. Papain nanoparticles synthesized in water and 50 mM phosphate buffer were irradiated at different dose rates of 0.8, 2, 5 and 10 kGy h^{-1} to reach the dose of 10 kGy.

2.2.2.3. Irradiation temperature. Nanoparticle synthesis was performed on ice bath and the samples were allowed to stabilize for one hour and 30 min at room temperature (20 ± 2 °C), ice bath (0 ± 2 °C) and cryogenic conditions (-20 ± 2 °C) prior to and maintained throughout the irradiation process performed at the dose rate of 5 kGy h^{-1}. Selected samples were prepared in deionized water and in 50 mM phosphate buffer.

2.2.3. Nanoparticle characterization

2.2.3.1. Nanoparticle size. Particle size was estimated by dynamic light scattering (DLS) on a Zetasizer Nano ZS90 device (Malvern Instruments, UK). All samples were analyzed at 20 °C and using a scattering angle of 173°. The measurements were performed in 3 sets of 10 runs of 10 s each in accordance with ISO 22412 (2017). The sizes were reported by number.

2.2.3.2. UV and bityrosine evaluation. The UV analysis was performed at wavelength (λ) of 280 nm on a SpectraMax i3 Multi-Mode Microplate Reader (Molecular Devices, USA). The samples were diluted in 50 mM phosphate buffer to reach equivalent absorbance prior to fluorescence studies. Bityrosine was evaluated by fluorescence on the same equipment using excitation wavelength (λ_{Ex}) of 350 nm, emission wavelength (λ_{Em}) scanning ranging from 350 to 500 nm, and excitation and emission bandwidths of 9 and 15 nm. Three scans were averaged for each spectrum.

2.2.3.3. Enzymatic activity. Papain proteolytic activity was quantified using Nα-benzoyl-DL-arginine-p-nitroanilide hydrochloride as a synthetic substrate. Samples were properly diluted in cysteine-versenne buffer (pH 7) and incubated on a thermostatic bath at 40 °C for 45 min. Absorbance was recorded at 405 nm on the above-mentioned microplate reader. The process was performed according to Ferraz et al. (2014).

2.2.3.4. pH. The pH measurements were performed at 20 °C using a SevenCompact S220 pH/Ion meter (Mettler Toledo, USA).

3. Results and discussion

Ionizing radiation has been proved an effective tool to promote protein-protein crosslinks for controllable particle size at nanoscale in a single step, as previously described by Queiroz et al. (2016) for BSA nanoparticles and Varca et al. (2014a, 2014b, 2016) for papain nanoparticles. The method involves the use of a cosolvent or desolvating agent such as ethanol to promote controlled aggregation of papain molecules prior to crosslinking for proper size distribution, as well as act as radioprotector due to the scavenging properties of ethanol (Panganamala et al., 1976; Phillisa et al., 1988). It has been demonstrated that the enzymatic activity loss was considerably low indicating that the process was suitable for synthesizing papain nanoparticles with preserved enzimatic activity (Varca et al., 2016).

According to recent studies (Muller et al., 2014; Dunnhaupt et al., 2015) papain has shown stability and biological affinity to be used as a nanocarrier. Among other advantages, the ability to overcome the mucosal and skin barrier, and avoid the rapid mucus clearance mechanism are highlighted (Dunnhaupt et al., 2015). In addition, authors like Beuth (2008) and Mohr and Desser (2013) reported that papain exhibits strong anti-angiogenic effects and demonstrated decreased tumor and therapy-induced side effects, therefore providing better quality of life of patients (Beuth, 2008).

Given the strong potential in terms of applications as nanocarrier for therapeutic agents, the proper control and knowledge over the radiation induced nanoparticle synthesis and crosslinking are essential for further use of the platform towards improved design and enhanced biological properties of the nanocarriers produced. Important parameters like papain and ethanol concentration and the effect of radiation dose have already been studied (Varca et al., 2014a, 2014b, 2016). The understanding of the influence and the role of parameters like buffer molarity, dose rate and irradiation temperature remain unclear and are the main themes of investigation in the present article.

3.1. The effect of buffer molarity

3.1.1. The influence of buffer molarity on the nanoparticles size

The standard procedure to produce papain nanoparticles was developed using 50 mM phosphate buffer at pH 7 (Varca et al., 2014a, 2014b, 2016). However, the effect of different buffer molarities on the nanoparticle formation has remained yet to be clarified. When nanopapain was synthetized at different buffer molarities, nanoparticle size

Table 1
The influence of the phosphate buffer molarity (1, 10, 25 and 50 mM) and deionized water on pH and papain nanoparticle size.

Condition	Native papain Size (d nm) ± Std. Dev/pH	Irradiated papain	Nanopapain
Water	3.6 ± 0.9/5.6	3.3 ± 0.8/5.2	8.0 ± 1.4/5.6
1 mM	4.1 ± 1.0/6.5	3.9 ± 0.9/5.4	8.0 ± 1.8/5.7
10 mM	4.2 ± 1.0/6.9	3.9 ± 1.0/6.7	8.9 ± 1.6/6.8
25 mM	4.4 ± 1.0/7.0	4.3 ± 1.2/6.9	8.2 ± 1.7/7.2
50 mM	3.7 ± 1.0/7.3	4.6 ± 1.1/7.3	9.3 ± 1.9/7.7

Papain nanoparticles were synthesized at 10 mg mL^{-1} on ice bath and maintained throughout the irradiation process to reach the dose of 10 kGy at a dose rate of 5 kGy h^{-1} using a ^{60}Co source. Samples were analyzed by DLS in 3 sets of 10 runs of 10 s using a scattering angle of 173°. pH measurements were performed at 20 °C.

was minimally affected by the change in molarity, as revealed in Table 1. Nanoparticle sizes were estimated by DLS as previously quoted.

The pH of the sample, on the other hand, changed considerably by the absence or the reduction in buffer molarity with pH ranging from 5.2 to 7.7 as registered for the nanoparticle synthesized in water and increased buffer molarity up to 50 mM. Changes of pH for non-irradiated and irradiated samples (especially in case of 1 mM solution) may indicate that buffer was directly involved in one of the reactions responsible for the formation of bityrosine crosslinks.

In deionized water nanoparticle size changed from 3.6 nm for native to 3.3 nm for irradiated and 8 nm for nanopapain within a pH ranging from 5.2 to 5.6. Such values were very similar to the pH of the deionized water, identified as 5.5. Nanoparticles synthesized at 1 and 10 mM showed a hydrodynamic diameter of 4.1 and 4.2 nm for native papain, 3.9 nm for the irradiated sample and 8.0–8.9 nm for nanopapain, with a pH ranging from 5.4 to 6.9, respectively. At 25 mM, native papain presented 4.3 nm, whereas 4.4 and 8.2 nm corresponded to irradiated and nanopapain sizes, with a pH of 6.9 and 7.2, respectively.

Samples synthetized at 50 mM buffer were considered the gold standard and presented a pH range around 7.3–7.7. Nanoparticle size was about 3.7 nm for native, 4.6 nm for the irradiated papain and 9.3 for nanopapain. Size differences were not considered relevant if the standard deviations were taken into account.

It is proper to say that buffer molarities did not alter nanoparticle size. However, the pH range may be an important parameter for further stages of development and the final applications, as well as other properties of the nanoparticle such as enzymatic activity. The pH change (through the reduction of molarity) of irradiated samples and nanopapain led to an increase in size of around 1 nm. For native papain, such increase did not seem to be related to pH. It is worth mentioning that a study regarding the influence of pH on nanoparticle formation should be addressed for a better clarification of the role of the buffer from both a nanoparticle synthesis and a stability approach.

3.1.2. *Buffer molarity over bityrosine formation*

The effects of the irradiation on proteins in aqueous solution occur mainly by the attack of free radicals generated from water radiolysis. This exposition leads to damage and depending upon the conditions may trigger the formation of bityrosine linkages (Bian and Chowdhury, 2014) of intra- or intermolecular nature, which contribute significantly to the conformation changes within a protein (Kar et al., 2017). The bityrosine formation occurs in 3 stages: hydrogen abstraction, isomerization and recombination (Giulivi et al., 2003).

Protein crosslinking levels by means of bityrosine may be estimated by fluorescence measurements using excitation and emission values set at λ_{ex} = 350 nm and λ_{em} = 375–500 nm, respectively. Bityrosine features a non-tryptophan profile with maximum fluorescence emission around 410–420 nm, depending upon the excitation wavelength. The fluorescence quenching for macromolecules like papain is analyzed by a change in the quantum yields of fluorescence from a fluorophore induced the by the novel crosslinks (Kar et al., 2017).

Bityrosine formation occurred in all samples regardless of buffer molarity. For a better comparison, the bityrosine levels registered for native papain were normalized to 1. The irradiated papain presented 1.8-fold increase and nanoparticles synthesized and irradiated at different buffer molarities and in deionized water presented the following increasing order of bityrosine formation: 10 and 25 Mm buffer (1.1

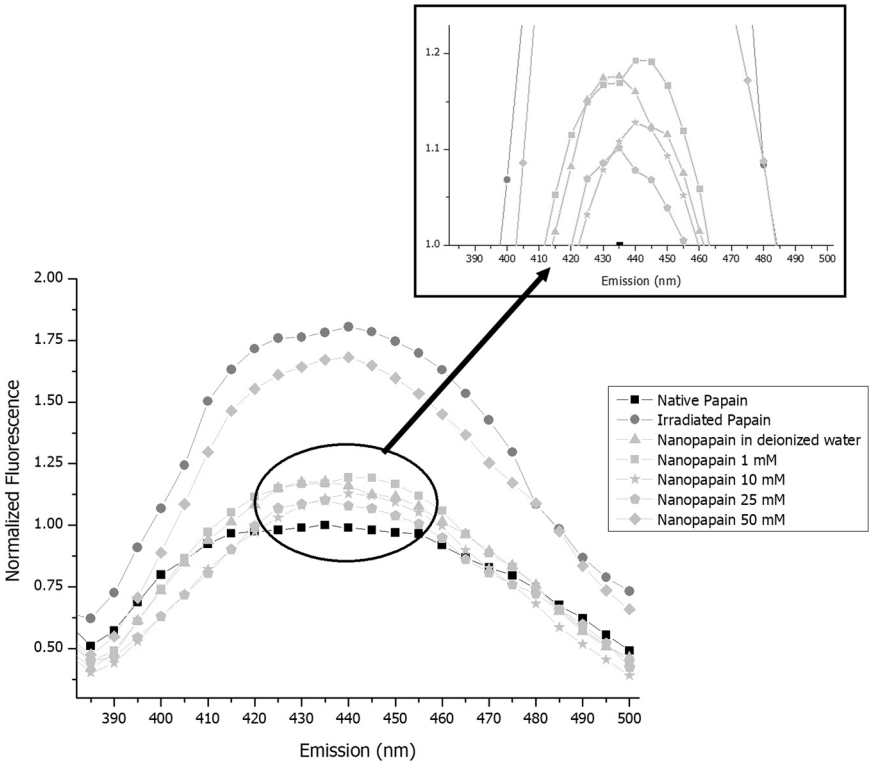

Fig. 1. Influence of phosphate buffer molarity (1, 10, 25 and 50 mM) and deionized water on bityrosine formation in papain nanoparticles. Nanoparticles were synthesized at 10 mg mL^{-1} on ice bath and maintained throughout the irradiation process to reach the dose of 10 kGy at a dose rate of 5 kGy h^{-1} using a ^{60}Co source. Samples were analyzed by fluorescence measurements using excitation wavelength (λ_{Ex}) of 350 nm and emission wavelength (λ_{Em}) scanning ranging from 350 to 500 nm, with excitation and emission bandwidths of 9 and 15 nm.

fold), deionized water and 1 Mm buffer (1.2 fold) and 50 Mm buffer (1.4 fold), as revealed in Fig. 1.

The contribution of the buffer molarity in the formation of bityrosine was evidenced by the intensity of the signal presented by the samples, as the highest values were registered at 50 mM. The mechanism involving bityrosine formation occurs via one-electron oxidation (Bobrowski et al., 2008), in which it was hypothesized that the electron would come from the buffer. Although as buffer molarity increased the bityrosine levels increased considerably, the formation of bityrosine was also observed when the process was carried out in water. This information highlights that the buffer molarity may impact bityrosine formation to an extent but is not mandatory for the crosslinking to occur. This also evidences that other linkages or pathways may also be related to the nanoparticle formation.

3.1.3. The effect of buffer molarity over the enzymatic activity

As previously described the proteolytic activity loss expected as a function of the specific irradiation processing for papain was around 20% (Varca et al., 2014a, 2014b, 2016) if compared to the native enzyme. The samples of interest, irradiated papain and nanopapain, showed relatively low bioactivity when synthesized and irradiated in water, with activity values ranging between 65% and 75% of the native (unirradiated) papain.

As shown in Fig. 2 samples synthesized at 1 mM phosphate buffer presented results similar to the gold standard (80% of bioactivity for nanopapain) and may be considered an option due the pH being 6, which corresponds to optimal pH for papain (Smith et al., 1955; Merck Index, 2006). At 10 and 25 mM, the enzymatic activity of nanopapain corresponded to approximately 70%, lower than expected for this condition. At 50 mM all samples presented enzymatic activity over 80% after irradiated process and therefore were considered the gold standard.

On the contrary, while size and bityrosine presented minor changes between samples, enzymatic activity showed that phosphate buffer molarity does play a relevant role in preserving enzymatic activity during the processing involved at the radiation dose rate of 5 kGy h^{-1}. However, it is important to mention that although there was experimental evidence of such influence, other parameters may also have impact on the biological activity. The presented results corroborated those previously reported by Varca et al. (2014a, 2014b, 2016).

The radiation induced inactivation of enzymes in solution is well known to occur via indirect effects of radiation, in which the attack by

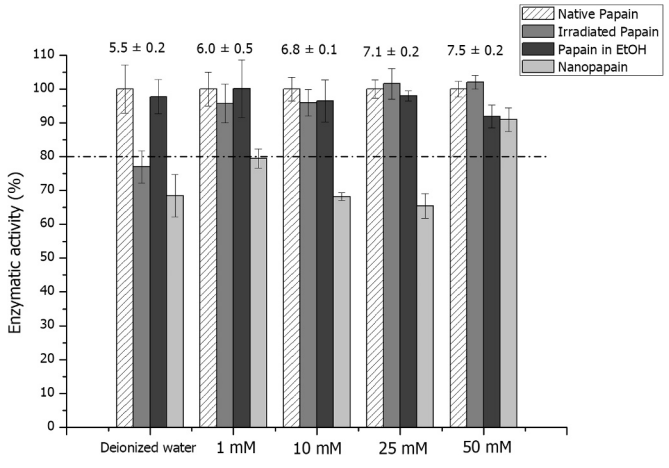

Fig. 2. The influence of deionized water and phosphate buffer molarity (1, 10, 25 and 50 Mm) on proteolytic activity of papain nanoparticles. Nanoparticles were synthesized at 10 mg mL^{-1} on ice bath and maintained throughout the irradiation process to reach the dose of 10 kGy at a dose rate of 5 kGy h^{-1} using a ^{60}Co source. Proteolytic activity was determined using BAPA as specific substrate at 40 °C and pH 7.

Table 2
The influence of radiation dose rate (0.8, 2, 5 and 10 kGy h^{-1}) on papain nanoparticle size.

Samples	Dose rate (kGy h^{-1})			
	0.8	2	5	10
Irradiated Papain (d nm)	3.5 ± 0.8	4.4 ± 0.9	3.9 ± 0.8	4.7 ± 0.9
Nanopapain (d nm)	7.1 ± 1.6	7.5 ± 1.8	7.9 ± 1.5	7.9 ± 1.6

Papain nanoparticles were synthesized at 10 mg mL^{-1} on ice bath and maintained throughout the irradiation process to reach the dose of 10 kGy at a dose rate of 5 kGy h^{-1} using a ^{60}Co source. Samples were analyzed by DLS in 3 sets of 10 runs of 10 s using a scattering angle of 173°.

free radicals resultant from solvent radiolysis may impact the enzymatic activity whether by impairment of substrate binding due to conformational changes or via direct modification of the active site (Saha et al., 1995). In the case of papain, the radiation induced oxidation of the cysteine-25, one of the amino acids that build up the active site (characteristic to cysteine proteases), stands as the most probable pathway for such inactivation.

3.2. Effect of irradiation parameters

3.2.1. The influence of dose rate over nanoparticle size

The effect of dose rate over papain nanoparticle formation was evaluated by exposing the samples to a γ-radiation dose of 10 kGy at different dose rates as demonstrated in Table 2. At 0.8 kGy h^{-1} the obtained particle sizes were about 3.5 nm for irradiated papain and 7.1 nm for nanopapain. At 2 kGy h^{-1} nanoparticle sizes were registered around 4.4 and 7.5 nm for irradiated and nanopapain respectively. At 5 and 10 kGy h^{-1} the hydrodynamic diameter was established as 3.9 and 4.7 nm for irradiated papain, respectively, and 7.9 nm for nanopapain at both dose rates.

In summary, the irradiation of papain for nanoparticle formation at different dose rates led to no relevant changes in particle size. All dose rates presented a similar size for irradiated papain (3.5–4.7 nm) and nanopapain (7–8 nm) with a minimum standard deviation of 0.8–1.8 nm, and thus evidencing that this parameter did not directly influence the nanoparticle size.

3.2.2. The influence of dose rate over bityrosine formation

The effects of dose rate over bityrosine formation were also assayed for all samples. Fluorescence profiles (Fig. 3) presented their typical behavior: irradiated papain > nanopapain > native papain, as reported by Varca et al. (2014a, 2014b). Samples irradiated at 0.8 kGy h^{-1} showed high bityrosine levels for irradiated papain of about 4.5-fold increase while nanopapain level was about 1.5-fold if compared to the levels observed for native papain.

At 2 kGy h^{-1}, the levels reached were 1.5-fold for irradiated papain and 1.3-fold for nanopapain. As for the nanoparticles irradiated at 5 kGy h^{-1} high level of bityrosine were achieved, considering 5 and 2.6-fold increase for irradiated and nanopapain, respectively. At 10 kGy h^{-1} **(**Fig. 3**D)**, irradiated papain presented a 2.6-fold increase, however nanopapain did not seem to undergo bityrosine crosslinking as the values were the same as those observed for the native sample.

The results indicated that samples irradiated at 0.8 kGy h^{-1} (Fig. 3**A**) and 5 kGy h^{-1} (Fig. 3**C**) presented higher levels of bityrosine emission than the other samples, with bityrosine levels reaching 4 and 5-fold increase, while at the other assayed conditions such values did not exceed a 3-fold increase. On the other hand, nanoparticles irradiated at 2 kGy h^{-1} (Fig. 3**B**) and 5 kGy h^{-1} (Fig. 3**C**) demonstrated formation of bityrosine at controlled levels, higher than native and lower than irradiated sample in absence of ethanol. In summary, the samples irradiated at 5 kGy h^{-1} were found to promote higher levels of

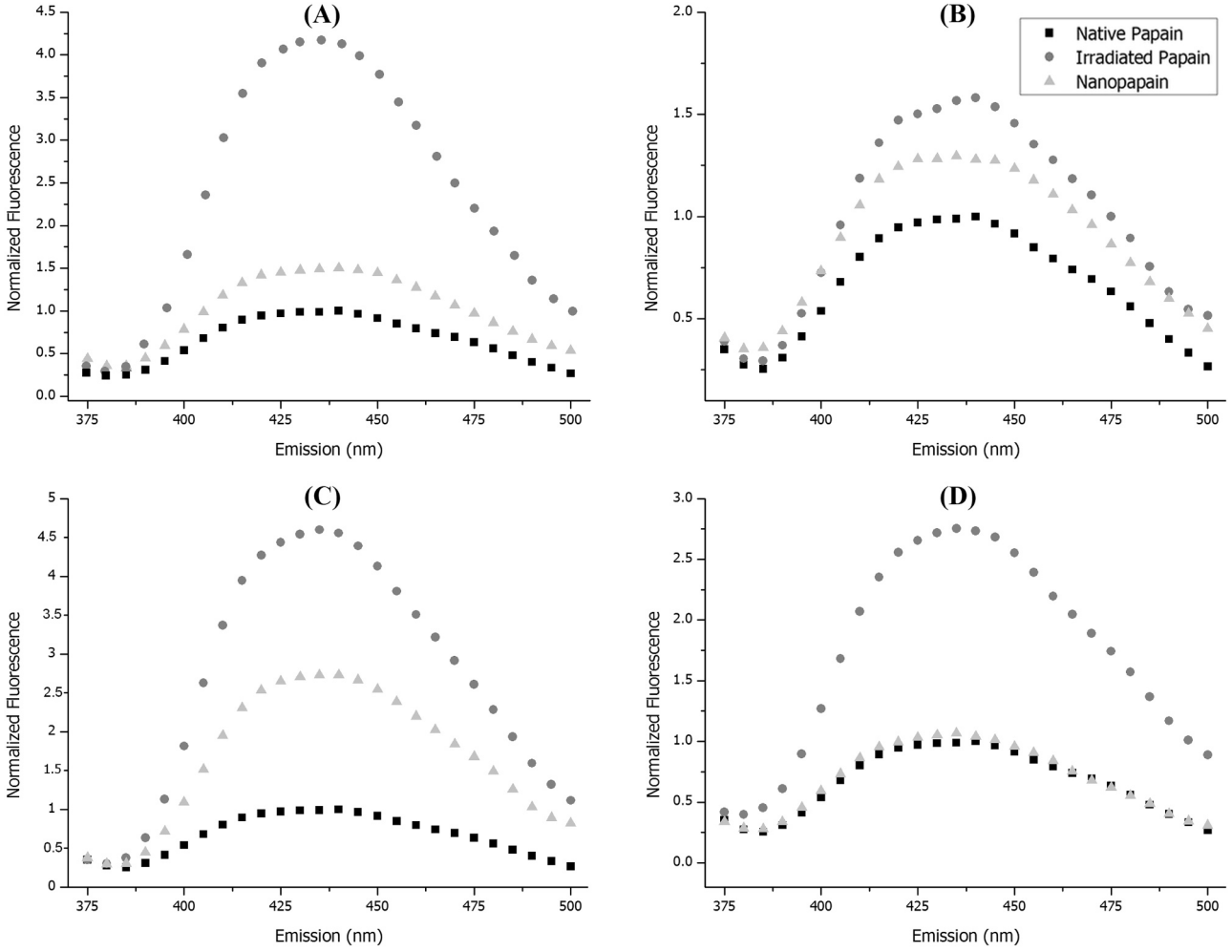

Fig. 3. The influence of radiation dose rate on bityrosine formation in papain nanoparticles irradiated at **(A)** 0.8 kGy h^{-1}, **(B)** 2 kGy h^{-1}, **(C)** 5 kGy h^{-1} and **(D)** 10 kGy h^{-1} using a ^{60}Co. Nanoparticles were synthesized at 10 mg mL^{-1} on ice bath and maintained throughout the irradiation process to reach the dose of 10 kGy. Samples were analyzed by fluorescence measurements using excitation wavelength (λ_{Ex}) of 350 nm and emission wavelength (λ_{Em}) scanning ranging from 350 to 500 nm with excitation and emission bandwidths of 9 and 15 nm.

bityrosine crosslinking and therefore this specific dose rate was considered the gold standard condition for bityrosine formation.

3.2.3. Dose rate effects on the enzymatic activity

Nanopapain was already studied in a dose range of 2.5–10 kGy at dose rates of 6.8 kGy min^{-1} and 1.2 kGy h^{-1} (Varca et al., 2014a, 2014b, 2016). The results showed that irradiation at both dose rates led to preserved bioactivity values placed around 75–80%. In the seek for a better understanding towards the effects of radiation dose rate over papain proteolytic activity, nanopapain and its controls were exposed to 10 kGy at 0.8, 2, 5 and 10 kGy h^{-1} and evaluated using BAPA as specific substrate.

Samples synthesized in deionized water and 50 mM phosphate buffer presented similar enzymatic activity values as demonstrated in Fig. 4. At 0.8 and 2 kGy h^{-1} the enzymatic activity levels remained close to 80% of the initial value. However, the samples irradiated at 5 kGy h^{-1} showed the lowest enzymatic activity loss among all dose rates evaluated, showing an enzymatic activity of about 90%. At 10 kGy h^{-1} the samples irradiated in both conditions – water and buffer showed the highest bioactivity loss.

Irradiated papain and papain in the presence of ethanol did not present significant enzymatic activity loss with values ranging from 0% to 10% enzymatic activity decay. Nanopapain in deionized water (Fig. 4**A**) and in 50 mM phosphate buffer (Fig. 4**B**) showed an enzymatic activity loss of about 20%, considering samples irradiated at 0.8, 2 and 5 kGy h^{-1}. Samples irradiated at 10 kGy h^{-1} demonstrated that this specific radiation dose rate led to nanoparticles with the highest bioactivity loss (about 30% of the initial one) amongst the dose rates assayed. In conclusion, the dose rate of 5 kGy h^{-1} was established as the most appropriate for the synthesis of the nanoparticles, which led to the highest activity values in a reduced processing time.

3.3. The role of temperature over the nanoparticle formation

3.3.1. Effects of irradiation temperature over the nanoparticle formation

To understand the effect of irradiation temperature, nanopapain was synthetized on ice bath and was allowed to rest for 1 h 30 min at temperatures of 20, 0 and − 20 °C and irradiated under the same conditions. Nanoparticle size wasn't affected by the temperature changes. In specific terms, it could be observed in Fig. 5 that the sizes and standard deviations for all conditions were practically the same and therefore implying that temperature did not influence the hydrodynamic size of the nanoparticle.

In fact, there is no dependence on temperature over radiation absorption, however the effectiveness of the damage over enzymes is hardly dependent on temperature through the radiation exposure (Vollmer and Fluke, 1967). However, as our results showed no differences in terms of size, this provides an experimental evidence that in

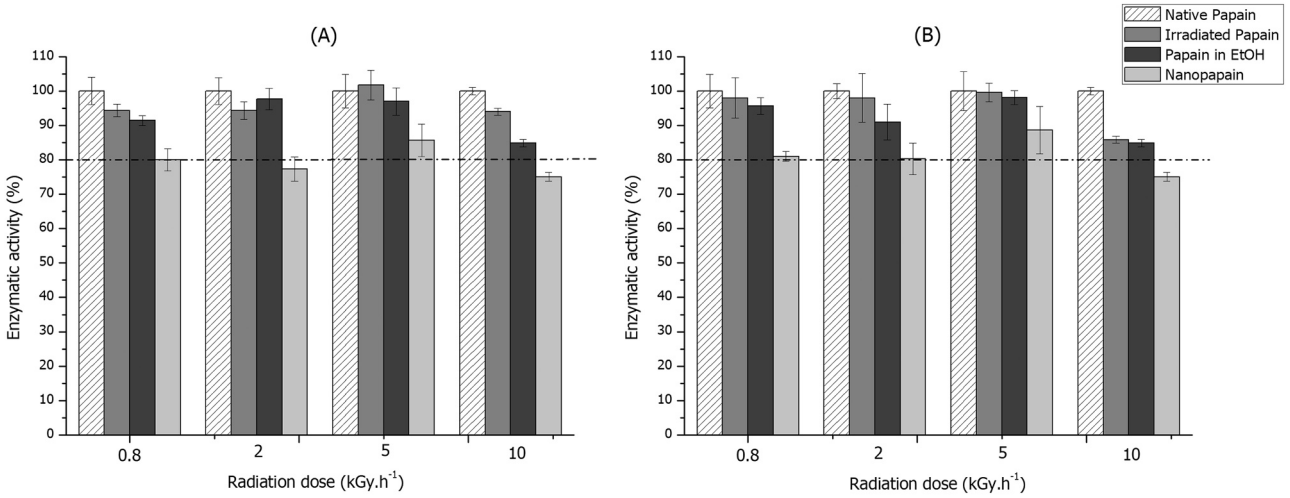

Fig. 4. The influence of radiation dose rate on proteolytic activity of papain nanoparticles irradiated at 0.8, 2, 5 and 10 kGy h^{-1} in **(A)** deionized water and **(B)** 50 mM phosphate buffer using a ^{60}Co. Nanoparticles were synthesized at 10 mg mL^{-1} on ice bath and maintained throughout the irradiation process to reach the dose of 10 kGy. Proteolytic activity was determined using BAPA as specific substrate at 40 °C and pH 7.

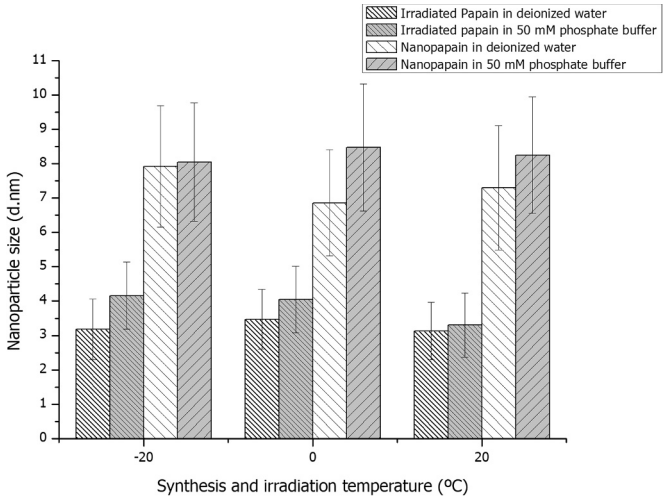

Fig. 5. The influence of synthesis and irradiation temperature on papain nanoparticle size. Papain nanoparticles were synthesized at 10 mg mL^{-1} on ice bath and maintained throughout the irradiation process to reach the dose of 10 kGy at a dose rate of 5 kGy h^{-1} using a ^{60}Co source. Samples were analyzed by DLS in 3 sets of 10 runs of 10 s using a scattering angle of 173°.

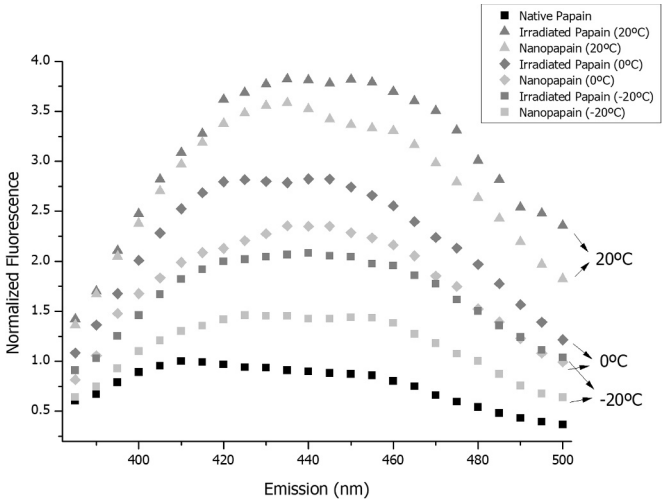

Fig. 6. The influence of synthesis and irradiation temperature on bityrosine formation in papain nanoparticles. Papain nanoparticles were synthesized at 10 mg mL^{-1} on ice bath and maintained throughout the irradiation process to reach the dose of 10 kGy at a dose rate of 5 kGy h^{-1} using a ^{60}Co source. Bityrosine was evaluated by fluorescence measurements using λ_{ex} = 350 and λ_{em} = 375–500.

the case of papain, the size increase is perhaps not a consequence of the irradiation exclusive, but rather a result of the ethanol effects or the combination of both.

3.3.2. The effects of temperature over bityrosine formation

Protein crosslinking by means of bityrosine formation increased as temperature increased. As reveled in Fig. 6 samples prepared at 20 °C showed bityrosine increase of 3–3.5-unit folds, while at zero degrees preparations led to 2-fold to 2.7-fold and at − 20 °C samples showed low bityrosine emission between 1.2-fold and 1.8-fold if compared to the native values. Therefore, as above mentioned, temperature may change the crosslinking levels and thus it is recognized as a relevant parameter for the control of the process (Hirschl et al., 2013).

The direct impact of temperature on bityrosine formation with no traceable changes in measured sizes, also correlates with our findings that bityrosine levels may not be directly related to the particle size increase, as claimed by our group in previous articles (Varca et al., 2016). This raises questions regarding the nature of such linkages, which unlikely observed for albumin (Queiroz et al., 2016) they are more likely to occur via intramolecular crosslinking rather than intermolecular one. More experiments should be carried out to confirm such hypothesis.

3.3.3. Effects of irradiation temperature over enzymatic activity

After irradiation, nanopapain samples tended to lose some of the enzymatic activity due to processing, in which about 20% loss of enzymatic activity was expected. As shown in Fig. 7, all samples synthetized and irradiated in deionized water at different temperatures presented an enzymatic activity higher than 80% for nanopapain.

Regarding enzymatic activity of the samples irradiated in 50 Mm buffer solution at 20, 0 and − 20 °C, it is proper to say that samples irradiated at ice-cold conditions held less bioactivity loss in comparison to the samples irradiated at room temperature, which was expected. However, as revealed in Fig. 6, crosslinking levels were inferior if compared to the same sample synthesized at 0 °C.

The obtained results prove that the optimal conditions for the synthesis would be to perform the process on ice bath, with

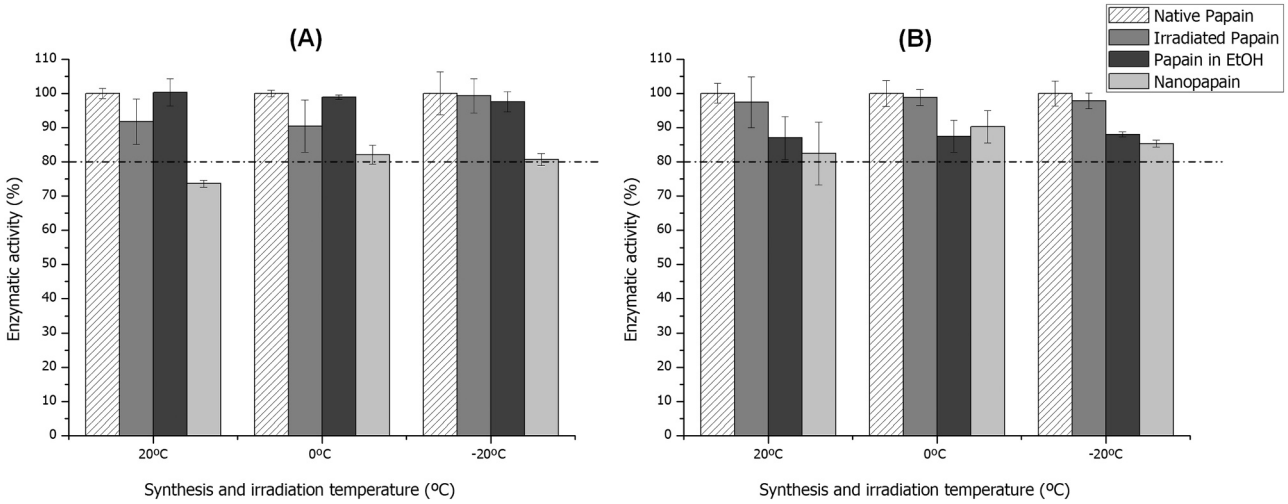

Fig. 7. The influence of synthesis and irradiation temperature on the proteolytic activity of papain nanoparticles in **(A)** deionized water and **(B)** 50 mM phosphate buffer using a ^{60}Co. Nanoparticles were synthesized at 10 mg mL^{-1} on ice bath and maintained throughout the irradiation process to reach the dose of 10 kGy. Proteolytic activity was determined using BAPA as specific substrate at 40 °C and pH 7.

temperature of 0 °C, using 50 mM phosphate buffer and a dose rate of 5 kGy h^{-1}. Such parameters were found to lead to the formation of papain nanoparticles without significant decay of the proteolytic activity while providing considerable crosslinking levels.

4. Conclusions

The synthesis of papain-based nanoparticles with the use of radiation-induced technique was performed through the solubilization of papain in phosphate buffer followed by the addition of ethanol as co-solvent and ^{60}Co as radiation source for gamma radiation (10 kGy) to promote protein crosslinking. This technique is a promising process to synthetize crosslinked papain nanoparticles and promote simultaneous sterilization and/or bio-reduction in a single step. The radiation-induced technique allows the sample to crosslink without significantly denaturing the enzyme. After evaluating all processing stages, this work advances the discussion in terms of achieving optimized parameters for nanoparticle synthesis.

Concerning the influence of buffer molarity over papain nanoparticle formation, nanoparticles size did not change significantly at the molarity range assayed, presenting a hydrodynamic diameter for native papain between 3.6–4.4 nm, 3.3–4.6 nm for irradiated protein and 8–9.3 nm for nanopapain. The differences observed among the samples were related to pH, which ranged from 5.2 for deionized water to 7.7 for 50 mM buffer. In addition, the fluorescence measurements confirmed the contribution of the buffer molarity in terms of bityrosine formation, as the highest signal was recorded for 50 mM buffer solution. On the other hand, while size presented minor change between samples, enzymatic activity showed that phosphate buffer molarities may play a relevant role in preserving enzymatic activity during processing. The results were random to some extent, but samples irradiated at 1 and 50 mM demonstrated less bioactivity loss than the other assayed samples. This could also be related to the pH variation, among other aspects.

Regarding the dose rates studied, all of them led to similar sized particles for irradiated papain (3–4 nm) and nanopapain (7–8 nm). Therefore, it was demonstrated that this parameter did not influence the formation of the particle size directly. The crosslinking levels, on the other hand, were evidenced by means of bityrosine formation and showed that samples irradiated at 0.8 and 5 kGy h^{-1} presented an increase in bityrosine levels of 4 and 5-folds while at other dose rates, 2 and 10 kGy h^{-1} specifically, the increase did not exceed 3-fold. As for enzymatic activity, it was verified that nanoparticles irradiated at both 0.8 and 2 kGy h^{-1} remained close to 80% of the initial bioactivity, whereas the nanopapain synthesized at 5 kGy h^{-1} showed the least enzymatic activity loss among all samples, featuring a residual enzymatic activity of 90%. At 10 kGy h^{-1} the enzymatic activity decreased to 70% of the initial one.

The influence of irradiation temperature on nanoparticles size was not observed, however fluorescence experiments demonstrated that more bityrosine crosslinks were formed as the temperature increased in the order of 20 > 0 > -20 °C. Concerning enzymatic activity, samples irradiated under ice-cold conditions presented decreased bioactivity loss, if compared to the samples irradiated at room temperature, while the lowest activity loss was registered at − 20 °C.

In conclusion, the optimized parameters for the synthesis of papain nanoparticles crosslinked by radiation were established as follows: 50 mM phosphate buffer at pH 7.4, dose rate of 5 kGy h^{-1} and 0 °C for sample preparation and irradiation temperature. In these conditions, the nanoparticle formation occurs faster than at the standardized conditions for synthesis, ensuring high proteolytic activity with relevant crosslinking levels.

As further points of studies the influence of pH over the papain nanoparticle formation and its impact over enzymatic activity and bityrosine formation remain to be clarified. The intramolecular or intermolecular nature of such linkages also require some further details for a better comprehension. In addition, stability monitoring and testing to verify optimum pH and temperature shall be addressed for a better understanding of the developed nanoparticles.

Acknowledgments

The authors would like to thank Centro de Tecnologia das Radiações (CTR – IPEN-CNEN/SP) for irradiating the samples and Instituto de Química (IQ – University of São Paulo) for the DLS analysis. Comissão Nacional de Energia Nuclear (CNEN) for scholarship, Sao Paulo Research Foundation FAPESP for a scholarship (No. 2015-13979-0). International Atomic Energy Agency IAEA (CRP F22064) Conselho Nacional de Desenvolvimento Cientifico e Tecnologico (CNPq) (project no. 402887/2013-1) for financial support.

References

Abdou, M., Abbas, O., 2009. Evaluation of diphenyl dimethyl bicarboxylate (DDB) as a probable hepato-protector in rats against whole body gamma irradiation. J. Biosci. Res. 6, 1–11.

Amri, E., Mamboya, F., 2012. Papain, a plant enzyme of biological importance. Am. J.

Biochem. Biotechnol. 8, 99–104.
Beuth, J., 2008. Proteolytic enzyme therapy in evidence-based complementary oncology: fact or fiction? Integr. Cancer Ther. 7, 311–316.
Bian, S., Chowdhury, S.M., 2014. Profiling protein-protein interactions and protein structures using chemical cross-linking and mass spectrometry. Austin J. Biomed. Eng. 1, 1017.
Bobrowski, K., Houée-Levin, C., Marcianiak, B., 2008. Stabilization and reactions of sulfur radical cations: relevance to one-electron oxidation of methionine in peptides and proteins. Chimia 62, 728–734.
Dunnhaupt, S., Kammona, O., Waldner, C., Kiparissides, C., Bernkop-Schnurch, A., 2015. Nano-carrier systems: strategies to overcome the mucus gel barrier. Eur. J. Pharm. Biopharm. 96, 447–453.
Ferraz, C.C., Varca, G.H.C., Vila, M.M.D.C., Lopes, P., 2014. Validation of in vitro analytical method to measure papain activity in pharmaceutical formulations. Int. J. Pharm. Pharm. Sci. 6, 658–661.
Fuchs, S., Coester, C.J., 2010. Protein-based nanoparticles as a drug delivery system: chances risks, perspectives. J. Drug Del. Sci. Technol. 20, 331–342.
Giulivi, C., Traaseth, N.J., Davies, J.K., 2003. Tyrosine oxidation products: analysis and biological relevance. Amino Acids 25, 227–232.
Grandishar, W.J., 2006. Albumin-bound paclitaxel: a next-generation taxane. Expert Opin. Pharmacother. 7, 1041–1053.
Hirschl, Ch, Biebl-Rydlo, M., DeBiasio, M., Muhleisen, W., Neumaier, L., Scherf, W., Oreski, G., Eder, G., Chernev, B., Schwab, W., Kraft, M., 2013. Determining the degree of crosslinking of ethylene vinyl acetate photovoltaic module encapsulants—a comparative study. Sol. Energy Mater. Sol. Cells 116, 203–218.
ISO, 2017. 22412:2017 – Particle size analysis – Dynamic light scattering (DLS).
Kamphuis, I.G., Kalk, K.H., Swarte, M.B.A., Drenth, J., 1984. Structure of papain refined at 1.65 Å resolution. J. Mol. Biol. 179, 233–256.
Kar, T., Basak, P., Ghosh, R.K., Bhattacharyya, M., 2017. Protective effects of curcumin against gamma ray induced conformational change of human serum albumin. Int. J. Biol. Macromol. 99, 600–607.
Lohcharoenkal, W., Wang, L., Cheng, Y.C., Rojanasakul, Y., 2014. Protein nanoparticles as drug delivery carriers for cancer therapy. BioMed. Res. Int (Article ID: 180549).
Merck Index, 2006. An Encyclopedia of Chemicals, Drugs, and Biologicals, 14 ed. Whitehouse Station, Merck, pp. 2564.
Mohr, T., Desser, L., 2013. Plant proteolytic enzyme papain abrogates angiogenic activation of human umbilical vein endothelial cells (HUVEC) in vitro. BMC Complement. Altern. Med. 13, 231.
Muller, C., Perere, G., Konig, V., Bernkshop-Schnurch, A., 2014. Development and in vivo evaluation of papain-functionalized nanoparticles. Eur. J. Pharm. Biopharm. 87, 125–131.
Panganamala, R.V., Sharma, H.M., Heikkila, R.E., Green, J.C., Cornwell, D.G., 1976. Role of hydroxyl radical scavengers, dimethyl sulfoxide, alcohols and methional in inhibition of prostaglandin synthesis. Prostaglandins 11, 599–607.
Phillisa, J.W., Esteveza, A.Y., O'Reganb, M.H., 1988. Protective effects of the free radical scavengers, dimethyl sulfoxide and ethanol, in cerebral ischemia in gerbils. Neurosci. Lett. 244, 109–111.
Queiroz, R.G., Varca, G.H.C., Kadlubowski, S., Ulanski, P., Lugão, A.B., 2016. Radiation-synthesized protein-based drug carriers: size-controlled BSA nanoparticles. Int. J. Biol. Macromol. 85, 82–91.
Saha, A., Mandal, P.C., Bhattacharyya, S.N., 1995. Radiation-induced inactivation of enzymes—a review. Radiat. Phys. Chem. 46, 123–145.
Sheldon, R.A., 2011. Characteristic features and biotechnological applications of cross-linked enzyme aggregates (CLEAs). Microbiol. Biotechnol. 92, 467–477.
Singh, D., Singh, R., 2012. Papain incorporated chitin dressings for wound debridement sterilized by gamma radiation. Radiat. Phys. Chem. 81, 1781–1785.
Smith, E.L., Finkle, B.J., Stockell, A., 1955. Some chemical and kinetic studies of crystalline papain. Discuss. Faraday Soc. 20, 96.
Tarhini, M., Greige-gerges, H., Elaissari, A., 2017. Protein-based nanoparticles: from preparation to encapsulation of active molecules. Int. J. Pharm. 522, 172–197.
Ulanski, P., Janik, I., Rosiak, J.M., 1998. Radiation formation of polymeric nanogels. Radiat. Phys. Chem. 52, 289–294.
Ulanski, P., Rosiak, J.M., 1999. The use of radiation technique in the synthesis of polymeric nanogels. Nucl. Instrum. Methods Phys. Res. Sect. 151, 356–360.
Varca, G.H.C., Ferraz, C.C.F., Lopes, P.S., Mathor, M.B., Grasselli, M., Lugão, A.B., 2014a. Radio-synthesized protein-based nanoparticles for biomedical purposes. Radiat. Phys. Chem. 94, 181–185.
Varca, G.H.C., Kadlubowski, S., Wolszczak, M., Lugão, A.B., Rosiak, J.M., Ulanski, P., 2016. Synthesis of papain nanoparticles by electron beam irradiation – a pathway for controlled enzyme crosslinking. Int. J. Biol. Macromol. 92, 654–659.
Varca, G.H.C., Perossi, G.G., Grasselli, M., Lugao, A.B., 2014b. Radiation synthesized protein based nanoparticles – a technique overview. Radiat. Phys. Chem. 105, 48–52.
Vollmer, R.T., Fluke, D.J., 1967. Temperature dependence of ionizing radiation effect on dry hyaluronidase. Radiat. Res. 31, 867–875.
Zarei, H., Bahreinipour, M., Eskandari, K., MousaviZarandi, S., Kaboudanian, A., 2017. Spectroscopic study of gamma irradiation effect on the molecular structure of bovine serum albumin. Vacuum 136, 91–96.